CHEMISTRY
A EUROPEAN JOURNAL

DOI: 10.1002/chem.201102260

Photoinduced Energy and Electron Transfer in Phenylethynyl-Bridged Zinc Porphyrin–Oligothienylenevinylene–C_{60} Ensembles

Maxence Urbani,[a] Kei Ohkubo,[b] D. M. Shafiqul Islam,[b] Shunichi Fukuzumi,*[b, c] and Fernando Langa*[a]

Abstract: Donor–bridge–acceptor triad (Por-2TV-C_{60}) and tetrad molecules ($(Por)_2$-2TV-C_{60}), which incorporated C_{60} and one or two porphyrin molecules that were covalently linked through a phenylethynyl-oligothienylenevinylene bridge, were synthesized. Their photodynamics were investigated by fluorescence measurements, and by femto- and nanosecond laser flash photolysis. First, photoinduced energy transfer from the porphyrin to the C_{60} moiety occurred rather than electron transfer, followed by electron transfer from the oligothienylenevinylene to the singlet excited state of the C_{60} moiety to produce the radical cation of oligothienylenevinylene and the radical anion of C_{60}. Then, back-electron transfer occurred to afford the triplet excited state of the oligothienylenevinylene moiety rather than the ground state. Thus, the porphyrin units in (Por)-2TV-C_{60} and $(Por)_2$-2TV-C_{60} acted as efficient photosensitizers for the charge separation between oligothienylenevinylene and C_{60}.

Keywords: electron transfer • energy transfer • fullerenes • oligothienylenevinylene • porphyrins • zinc

Introduction

The development of artificial photosynthetic systems that use solar energy would be a major advance in energy production and a critical breakthrough with respect to the growing concern of environmental pollution caused by the use of fossil fuels.[1] Typical designs of such systems have tried to mimic natural photosynthesis, such as the efficient capture of photons of visible light and electron/hole separation by electron transfer. In this respect, nanomaterials that are composed of multiporphyrins and carbon-based π-electron acceptors (in particular C_{60}) have been utilized to construct efficient light-energy conversion systems, such as photovoltaic devices.[2]

Porphyrins, which are characterized by their high molar absorption coefficients and which give fast energy and/or electron transfer to acceptor components in synthetic analogues of natural chlorophyll molecules, have been widely used as promising candidates for light-capturing chromophores.[3,4,5] The structural complexity of light-harvesting antenna complexes (LH1 and LH2) has prompted the design and preparation of light-harvesting multiporphyrin systems.[4,5] Fullerenes have also been widely used as 3D electron acceptors, owing to their small reorganization energy in electron-transfer reactions, which results from the π-electron system being delocalized over the curved 3D surface, together with the rigid and confined structure of the aromatic π-sphere.[3a–f, 6,7] The introduction of conjugated systems that act as bridges (B) between the donor (D) and the acceptor (A) mediates the energy-transfer and electron-transfer processes.

Oligophenylenevinylenes, oligophenyleneethynylene, and heterocyclic oligomers, such as oligothiophenes, oligofurans, and oligopyrroles, have been widely used as wires to connect D and A moieties.[8,9] However, the detailed role of oligothienylenevinylenes[9] as bridges in terms of energy transfer versus electron transfer has yet to be scrutinized.

Herein, we report the synthesis, electrochemical, and photodynamic studies of a porphyrin-2TV-C_{60} triad and a $(porphyrin)_2$-2TV-C_{60} tetrad together with reference compounds. Several factors were considered for designing this system: 1) an adequate gradient of the oxidation potentials, 2) thienylvinylenes[9] and phenylethynyl linkers[10] have well-known efficiency as molecular wires, and 3) the porphyrin core and phenylene planes are orthogonal, thereby breaking the conjugation between them. Photoinduced energy transfer and electron-transfer processes were investigated by using fem-

---

[a] Dr. M. Urbani, Prof. Dr. F. Langa
Instituto de Nanociencia
Nanotecnología y Materiales Moleculares (INAMOL)
University of Castilla-La Mancha Campus
de la Fábrica de Armas, Toledo 45072 (Spain)
E-mail: Fernando.Langa@uclm.es

[b] Dr. K. Ohkubo, Dr. D. M. S. Islam, Prof. Dr. S. Fukuzumi
Department of Material and Life Science
Graduate School of Engineering
Osaka University and ALCA
Japan Science and Technology Agency (JST)
2-1 Yamada-oka, Suita, Osaka 565-0871 (Japan)
Fax: (+81) 6-6879-7370
E-mail: fukuzumi@chem.eng.osaka-u.ac.jp

[c] Prof. Dr. S. Fukuzumi
Department of Bioinspired Science
Ewha Womans University
Seoul, 120-750 (Korea)

Supporting information for this article, including the synthesis and physical measurements, is available on the WWW under http://dx.doi.org/10.1002/chem.201102260.

tosecond and nanosecond laser flash photolysis measurements tougher with their redox properties.

Results and Discussion

Synthesis: The synthesis of 2TV building blocks is shown in Scheme 1. Phosphonates **1** and **2** were prepared from 3,5-dibromo benzaldehyde and 4-bromobenzyl bromide, respectively, according to literature procedures.[11] The reaction of phosphonate **1** with 2TV-aldehyde[12] in THF in the presence of *t*BuOK under Wittig–Horner conditions stereoselectively afforded the *trans-trans* isomer (*E*,*E*)-**3** in good yield (69 %). Surprisingly, the reaction of phosphonate **2** under the same conditions afforded compound **6**, but as an *E*/*Z* isomeric mixture; this result prompted us to perform the *Z*→*E* isomerization of compound **6**, by treatment with a catalytic amount of iodine in refluxing toluene, to yield isomer (*E*,*E*)-**6** in 79 % yield.

Our first attempt to directly functionalize compound **6** with (trimethylsilyl)acetylene (TMSA) by Sonogashira coupling failed, and mainly led to a mixture of the mono- (major) and bis-ethynyl (minor) products, presumably owing to the poor reactivity of *m*-bis-bromophenyl **6**. To increase their reactivities toward Sonogashira coupling, compounds **3** and **6** were first formylated by using a Vilsmeyer procedure in the presence of $POCl_3$ (1.3 equiv)/DMF (2–3 equiv) in refluxing DCE overnight to afford isomers (*E*,*E*)-**4** and (*E*,*E*)-**7**, respectively, with high *trans*-stereoselectivity (*E*,*E*/*Z*,*E*, about 90 %).[13] However, in these cases, *Z*→*E* isomerization of the mixtures could not be achieved by treatment with catalytic iodine, which mainly led to degradation products, presumably owing to the presence of the aldehyde group. However, the ratios of the *trans–trans* isomers were significantly increased (up to 96 %) after purification by column chromatography on silica gel and low-temperature recrystallization in *n*-pentane. Compounds **4** and **7** were finally obtained in 83 and 66 % yield, respectively. Activated bromophenyl compounds **4** and **7** were then subjected to Sonogashira coupling with TMSA, thereby affording the desired silyl-protected derivatives in good to acceptable yields. Full cleavage of the terminal alkyne units was then achieved by treatment with potassium carbonate in THF/MeOH (1:1). Compound **5** was isolated in excellent yield (99 %) after column chromatography on silica gel. However, several recrystallizations at low temperature were necessary to isolate the pure *trans* isomer (*E*,*E*)-**5** (*E*,*E*/*Z*,*E*, >98 %)[13] thus leading to a significant decrease in the yield (61 %, 2 steps from compound **4**). In the case of compound **8**, the *trans* isomer was isolated more easily (*E*,*E*/*Z*,*E*, >99 %).[13] However, many careful and tedious purification steps were required to separate the bis-alkyne precursor ((*E*,*E*)-**8a**) from the by-product ((*E*,*E*)-**8b**), which we were unable to fully isolate. We were able to improve the ratio of (*E*,*E*)-**8a/8b** up to 77:23[13] in the purest sample. The overall yield of compound **8a** was estimated to be 47 % in 2 steps from (*E*,*E*)-**7** (based on the effective amount of compound **8a** in the 77:23 mixture). The introduction of the terminal aldehyde functional group into compounds **3** and **6** to obtain aldehydes **4** and **7**, before coupling the porphyrins, was crucial at this stage because unformylated (2TV) bromophenyl derivatives **3** and **6** were poorly reactive toward Sonogashira coupling (with TMSA and por-

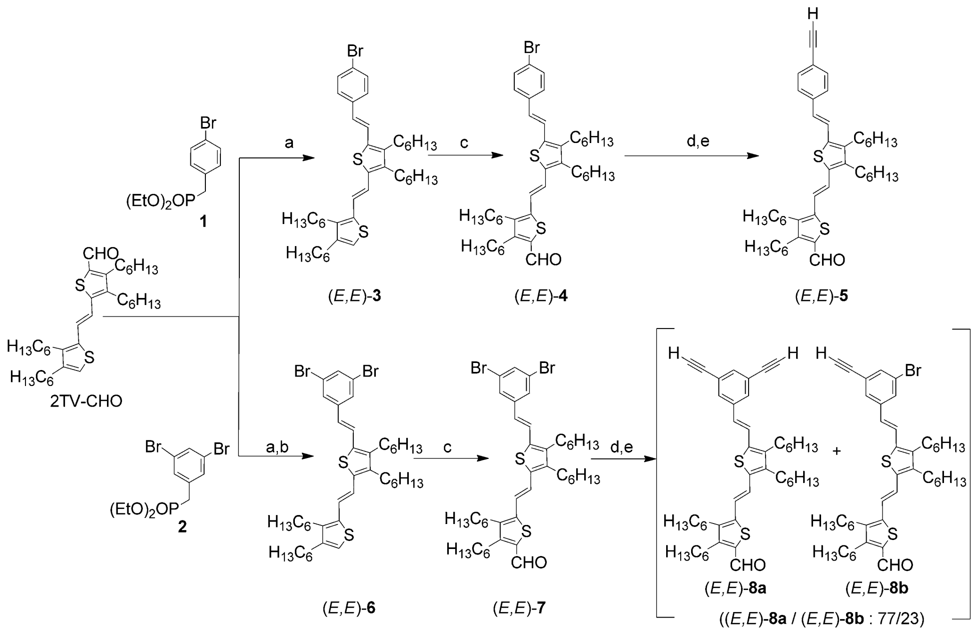

Scheme 1. Synthesis of 2TV building blocks, reagents and conditions: a) *t*BuOK, THF, 0 °C→RT 2 h ((*E*,*E*)-**3**: 69 %); b) I_2 (cat.), toluene, 6 h ((*E*,*E*)-**6**: 79 %); c) $POCl_3$ (1.3 equiv)/DMF (2–3 equiv), DCE, reflux, overnight ((*E*,*E*)-**4**: 83 %; (*E*,*E*)-**7**: 66 %); d) TMSA, [Pd(PPh_3)$_4$], CuI, Et_3N, RT, 24–48 h; e) K_2CO_3, THF/MeOH (1:1), RT, 8 h ((*E*,*E*)-**5:** 62 %; (*E*,*E*)-**8a/8b**: 82 %, two steps). DCE = 1,2-dichloroethane, DMF = *N*,*N*-dimethylformamide, TMSA = trimethylsilylacetylene.

phyrins). Then, because porphyrins are reactive under Vilsmeyer conditions, their undesired formylation side-reactions were avoided.

Synthetic approaches to prepare triad **11** and tetrad **12**, as well as their respective porphyrin precursors **9** and **10**, are shown in Scheme 2 and Scheme 3. The preparation of porphyrins **9** and **10** involved the Cu-free Pd-catalyzed cross-coupling of building blocks (*E*,*E*)-**5** or (*E*,*E*)-**8a**/**8b** with A_3B-type zinc porphyrin PZnI [5-*p*-iodophenyl-10,15,20-tris-(2,4,6-trimethylphenyl)zinc porphyrin][14] under the conditions optimized by Lindsey for the synthesis of ethyne-linked, multiporphyrin arrays.[15] Pure bis-adduct aldehyde (*E*,*E*)-**10** was isolated in 89 % yield (with respect to (*E*,*E*)-**8a**) after purification by size-exclusion chromatography and column chromatography on silica gel. By following the same procedure, pure (*E*,*E*)-**9** was isolated in 66 % yield.

The incorporation of C_{60} was achieved by the [3+2] dipolar cycloaddition with azomethine ylides that were generated in situ from aldehydes **9**/**10** and sarcosine in refluxing chlorobenzene, according to the procedure described by Prato and Maggini;[16] triad **11** and tetrad **12** were formed in 81 % and 49 % yield, respectively (Scheme 3). The structures of compounds **11** and **12** were confirmed by MS (MALDI-TOF, see the Experimental Section and the Supporting Information, Figures SI.11 and SI.12).

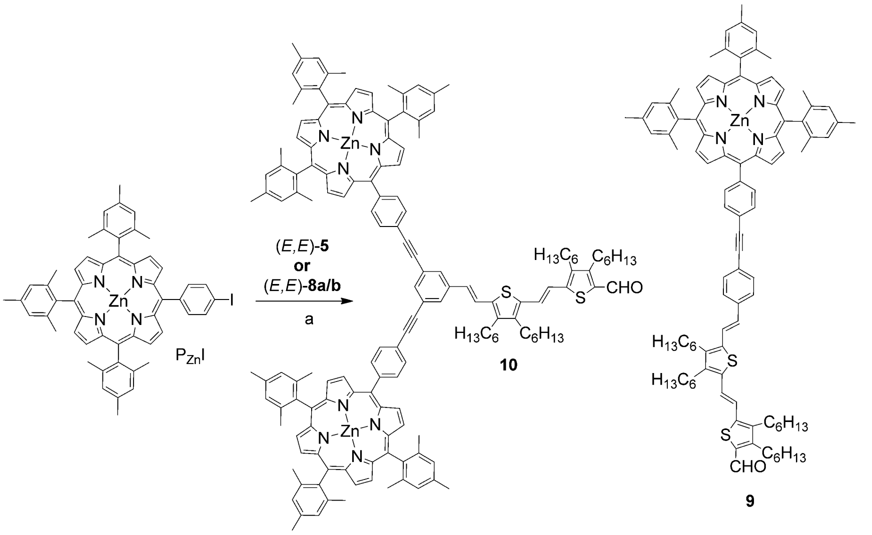

Scheme 2. Synthesis of Por-2TV (**9**) and $(Por)_2$-2TV (**10**), reagents and conditions: a) $AsPh_3$, $[Pd_2(dba)_3]$, Et_3N/toluene (1:5), 3 days (from (*E*,*E*)-**5**, **9**: 66 %; from (*E*,*E*)-**8a**/**8b**, **10**: 89 % based on (*E*,*E*)-**8a**). dba = dibenzylideneacetone.

Characterization of these compounds was achieved by NMR and UV/Vis spectroscopy. ^1H NMR spectra of compounds **11** and **12** are shown in Figure 1 (for compounds **3**–**10**, see the Supporting Information).

Derivatives **3**–**12** all displayed simple, well-resolved average NMR spectra at room temperature that were in agreement with their structures. The presence of a stereogenic center in the pyrrolidine rings of compounds **11** and **12** induced an asymmetric center (C1 symmetry) and involved two enantiomeric forms (*R* and *S*). Interestingly, all of these compounds showed much-simpler NMR spectra than expected owing to fast dynamic phenomena at room temperature. First, for all of the *para* derivatives (**3**, **4**, **5**, **9**, and **11**), an AB quartet was always clearly observed for the *para*-substituted phenyl-ring protons ($H_{X/Y}$). This observation indicated that exchange between the H_X/H_Y and $H_{X'}/H_{Y'}$ protons was always fast at 298 K on the NMR timescale (Scheme 4a) such that they appeared equivalent in the ^1H NMR spectrum. In other words, the rotation around the C–C bond that linked the 2TV moiety to the central phenyl core was faster than the NMR timescale at 298 K (fast rotation 1, Scheme 4a). Next, an AB quartet ($H_{o/m}$) was observed for the *para*-substituted bridging phenyl ring in the ^1H NMR spectra of compounds **9** and **11**, which indicated fast exchange between the $H_{o/m}$ and $H_{o'/m'}$ protons. Obviously, in this latter case, the fast exchange could also be explained by a fast rotation around the carbon–carbon triple bond (rotation 2, Scheme 4c). Although in principle the β-pyrrolic protons in compound **11** should lose their equivalency owing to the presence of the fulleropyrrolidine moiety, an "A_3B-type porphyrin" pattern was observed for both derivatives **9** and **11**, as attested to by the signals from the porphyrin moiety: an AB quartet and a singlet were observed

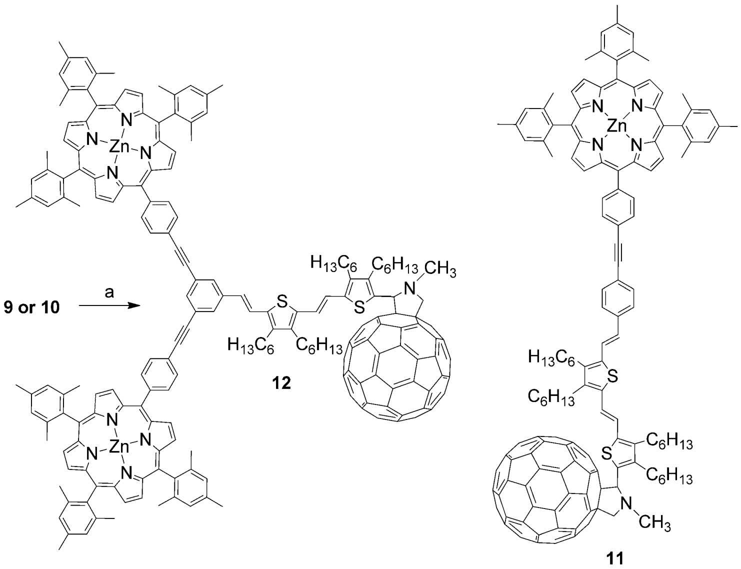

Scheme 3. Synthesis of Por-2TV-C_{60} (**11**) and $(Por)_2$-2TV-C_{60} (**12**), reagents and conditions: a) C_{60}, sarcosine, PhCl, reflux, 12 h (from **9**, **11**: 81 %; from **10**, **12**: 49 %).

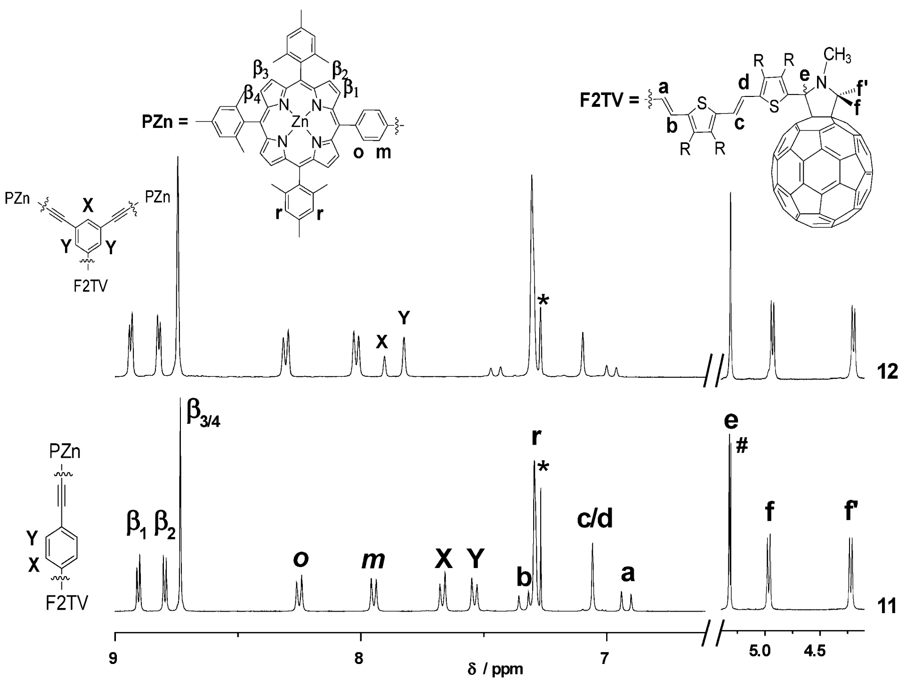

Figure 1. ^{1}H NMR spectra ($CDCl_3$, 400 MHz) of Por-2TV-C_{60} (**11**) and $(Por)_2$-2TV-C_{60} (**12**) (* denotes the residual $CHCl_3$ solvent peak, # denotes CH_2Cl_2).

for the four sets of β-pyrrolic protons (β_1/β_2 and β_3/β_4 respectively).

Similar observations and conclusions were drawn for the corresponding *meta* derivatives (**6**, **7**, **8**, **10**, and **12**). First, an AX_2 system for the 1,3,5-trisubstituted phenyl ring protons ($H_{X/Y}$) was clearly observed in all cases, which attested to a fast exchange between the H_Y and $H_{Y'}$ protons (Scheme 4b). Interestingly, the *para*-substituted ($H_{o/m}$) protons on the bridging phenyl rings of compounds **10** and **12** also only displayed one unique AB quartet. This observation attested to a fast exchange between the H_o/H_m and $H_{o'}$/$H_{m'}$ protons on one hand, and between the two phenyl bridging phenyl rings on the other hand. This result was also evidenced by the signals of the porphyrin moiety in compounds **10** and **12**: an AB quartet and a singlet were observed for the four sets of β-pyrrolic protons (β_1/β_2 and β_3/β_4, respectively). This latter observation attested to a fast exchange between the two inequivalent porphyrins PZn and PZn′ of compound **12**, which appeared to be magnetically equivalent to each other in the ^{1}H NMR spectra. We concluded from these NMR spectra that both fast rotations 1 and 2 occurred in *meta* derivatives **10** and **12** and one could reasonably suppose that should also both take place for the corresponding *para* derivatives (**9** and **11**). APT ^{13}C NMR experiments (see the Supporting Information) of compounds **11** and **12** revealed two unique, characteristic signals for the sp ethynyl carbons ($\delta = 90.7$ and 90.6 ppm for compound **11**; $\delta = 90.3$ and 89.6 ppm for compound **12**), which agreed with this hypothesis.

Finally, the steric hindrance that arose from the bulky *ortho*-hexyl chains on the thiophene that was directly linked to the pyrrolidine ring should induce a restricted rotation around the thiophene–pyrrolidine bond. Such phenomena are well-known and have been observed in the case of phenyl-substituted pyrrolidinofullerene derivatives.[17] Nevertheless, to the best of our knowledge, such phenomena have not been heavily investigated nor discussed in depth for thiophene-based derivatives. In principle, compounds (*R*/*S*)-**11** and (*R*/*S*)-**12** may exist as two sets of diastereoisomeric conformers (α and β; Figure 2). However, NMR spectroscopy seemed to indicate that only one atropoisomer existed at 298 K. Indeed, the NMR spectra of fullerene derivatives **11** and **12** displayed sharp, well-defined signals at room temperature. In particular, the signals of the vinylic protons of the 2TV moiety appeared as a unique AB quartet and a singlet

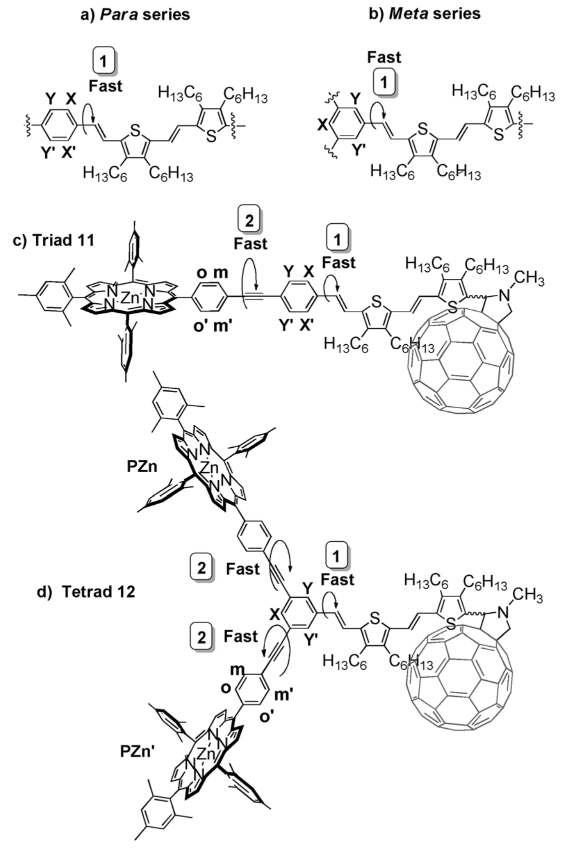

Scheme 4. Fast dynamic exchanges at 298 K and ^{1}H nomenclature of the phenyl bridging rings in a) the *para* series, b) the *meta* series, c) triad **11**, and d) tetrad **12**.

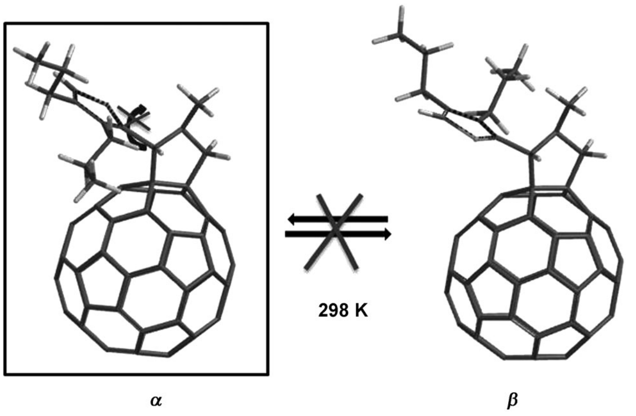

Figure 2. Energy-minimized equilibrium geometry of the C_{60}–thiophene fragment: theoretical structure of the two lowest-energy conformers (α and β) in the ground state (298 K). Calculations were performed with Spartan 10 by using the "conformer distribution" semiempirical PM3 method. The hexyl chains were replaced by propyl groups in the calculations (only the *R* enantiomer is shown).

for the two sets of *trans*-coupled vinylic protons $H_{a/b}$ ($J(a,b) \approx 16$ Hz) and $H_{c/d}$, respectively. Moreover, one unique AB quartet for protons $H_{f/f'}$ and a singlet for the H_e proton were observed for the pyrrolidine ring. In addition, APT ^{13}C NMR spectroscopy of compounds **11** and **12** revealed two signals for the sp^3 carbons of the C_{60} mono-adducts ($\delta =$ 70.0 and 68.8 ppm for compound **11**; $\delta = 70.0$ and 68.9 ppm for compound **12**; see the Supporting Information). From these experimental NMR observations, two hypotheses could be raised: either the rotation around the thiophene–pyrrolidine bond was faster than NMR timescale at room temperature (i.e., fast equilibrium between the α and β atropoisomeric forms) or that the rotation was fully restricted (based on NMR observations, this hypothesis would imply that only one atropoisomer existed at 298 K). This latter hypothesis was the most likely, as it is well-known that steric hindrance that arises from any bulky group located at the *ortho* position of the pyrrolidine ring induces a high rotational energy barrier that is sufficient to prevent any rotation around the pyrrolidine ring at 298 K.[17] Therefore, it was reasonable to suggest that the cycloaddition reactions on the fullerene core were highly diastereoselective, thereby leading to only one atropoisomer, in agreement with other examples previously reported in the literature.[17b,c] To determine which diastereoisomer was present, we performed semi-empirical computational studies on a fulleropyrrolidine–thiophene fragment by using different alkyl groups (methyl, ethyl, or propyl; Figure 2). The difference in energy between the α and β isomeric forms was estimated to be 5.6 kJ mol^{-1}(methyl), 7.3 kJ mol^{-1} (ethyl), and 7.6 kJ mol^{-1} (propyl). These results, together with computational studies of compounds **11** and **12** (semi-empirical PM3 method; see the Supporting Information, Figure SI.22–SI.31), both agreed that the α-atropoisomeric forms were the lowest-energy conformers (in which the hexyl chains were located on the same side as the H_e proton of the pyrrolidine ring). However, the difference in energy was rather too small to fully explain why only one isomer had been formed under these experimental conditions (chlorobenzene, 120 °C). Apart from steric hindrance considerations, other factors could also contribute to the high diastereoselectivities for compounds **11** and **12**. Additional energetic factors and/or dipolar-moment effects may also be heavily involved in the stabilization of the in-situ-generated azomethine ylide intermediates in chlorobenzene. As we had previously suggested and observed for other [C_{60}]pyrrolidine–*n*TV derivatives, the stabilization of the intermediate by π–π stacking between the C_{60} curved cage and the π-aromatic backbone of 2TV should play an important role.[18]

The redox behavior of compounds **11** and **12**, as well as their precursors (**5** and **8a**/**8b**–**10**) and reference compounds (porphyrin PZnI and C_{60}), were investigated by cyclic voltammetry (CV) and by Osteryoung square-wave voltammetry (OSWV) in ODCB/MeCN (8:2) at room temperature (for the CVs, see the Supporting Information, Figure SI.6; for the OSWVs, see the Supporting Information, Figure SI.7). The chemical reversibility (or irreversibility) of these redox processes and the number of electrons engaged (where possible) were deduced from CVs experiments. Owing to irreversible oxidation processes of 2TV-based derivatives, all redox potentials (versus Fc/Fc^+) were systematically deduced from OSWV experiments (Table 1).

Table 1. Redox potentials of compounds **5**, **8**–**12**, C_{60}, and [5-*p*-iodophenyl-10,15,20-tris-(2,4,6-trimethylphenyl)porphyrin] measured by OSWV (versus Fc/Fc^+).[a]

	E_{red2} [V]	E_{red1} [V]	E_{ox1} [V]	E_{ox2} [V]	E_{ox3} [V]
$P_{Zn}I$	−2.33	−1.93	0.35	0.73	–
5	–	–	0.52[b]	0.77[b]	–
8	–	–	0.52[b]	0.78[b]	–
9	–	−1.33	0.33	0.53[b]	0.74
10	–	−1.37	0.31 (br)	0.58[b]	0.90 (br)
11	−1.50	−1.10	0.36	0.71	0.90 (br)[b]
12	−1.37	−1.09	0.35	0.74	0.94 (br)[b]
C_{60}	−1.35	−0.99	–	–	–

[a] 0.20 M Bu_4NClO_4, solvent: ODCB/MeCN (8:2). [b] Irreversible according to CV. ODCB = 1,2-dichlorobenzene.

In the cathodic region, the first reduction wave of fulleropyrrolidine derivatives **11** ($E_{red1} = -1.10$ V) and **12** ($E_{red1} = -1.09$ V) was assigned to the first reversible reduction of the fullerene core through a one-electron process. The saturation of one of their C_{60} double bonds resulted in a cathodic shift of their reduction potentials ($\Delta V \approx -0.10$ V) in comparison with unsubstituted C_{60} ($E_{red1} = -0.99$ V). These values were in agreement with those previously reported for other similar fulleropyrrolidine–2TV derivatives, in particular those reported by Roncali et al.[9a,19] for a C_{60}-2TV system ($E_{red1} = -1.08$ V) and by ourselves for a C_{60}-2TV-C_{70} dumbbell ($E_{red1} = -1.30$ V).[18] At lower cathodic potentials, porphyrin macrocycle(s) showed a first (reversible) and a second (irreversible) reduction that involved one-electron processes for PZnI, Por-2TV-CHO (**9**), and Por-2TV-C_{60}

(**11**), and two-electron processes for $(Por)_2$-2TV-CHO (**10**) and $(Por)_2$-2TV-C_{60} (**12**). In these latter cases, both porphyrin moieties appeared to be reduced simultaneously. Interestingly, the first reduction of the porphyrin(s) in reference compounds **9** ($E_{1red} = -1.33$ V) and **10** ($E_{1red} = -1.37$ V) were positive-shifted by about +0.4 V compared to model porphyrin PZnI ($E_{1red} = -1.93$ V), which could be due to the presence of the ethynyl-2TV-CHO bridge. The second reduction potential peak in compounds **11** ($E_{red2} = -1.50$ V) and **12** ($E_{red2} = -1.37$ V) was more difficult to assign because both the reduction of the porphyrin(s) and other reductions of C_{60} may overlap. However, we could clearly conclude that the reductions of porphyrin(s) in compounds **11** and **12** occurred at lower potentials than the first reduction of the C_{60} moiety.

In the anodic region, two reversible oxidations at around +0.35 V and +0.73 V were clearly observed for the porphyrin moieties of PZnI and compounds **9**–**12** without any significant changes. Only small negative shifts (30–40 mV) were observed for compounds **9** and **10**, which could be due to the weak effect of the terminal aldehyde group. These results suggested that the electron transfer from the porphyrin moiety must be located on the macrocycle ring. For $(Por)_2$-2TV-CHO (**10**) and $(Por)_2$-2TV-C_{60} (**12**), only two oxidation processes were observed for the porphyrins. These results suggested that both porphyrin moieties in compounds **10** and **12** were equivalent from an electrochemical point of view, thus involving two-electrons for each of the two-electron-oxidation processes. This result was also evidenced in the cathodic region, where the reductions of both porphyrins also occurred simultaneously in two-electron processes (although in the case of compound **12**, they were more difficult to distinguish, owing to the overlap with the reductions waves that arose from the fullerene moiety). CVs of 2TV-based derivatives **5** and **8a**/**8b** showed two irreversible one-electron-transfer oxidation processes. In particular, two well-defined oxidation waves were clearly observed in the forward scan but became poorly defined when the potential was inverted (backward scan). It has been previously reported that the oxidation of short oligothienylenevinylene derivatives ($n < 4$) leads to the formation of *n*TV radical cation species, usually followed by fast electropolymerization on the electrode surface. However, the absence of any free α positions on the thiophene moieties, together with the presence of pendant hexyl chains, tended to avoid, or at least slow down, these electropolymerization processes.[12] OSWV clearly revealed two half-wave oxidations peaks for compounds **5** ($E_{ox1} = +0.52$ V; $E_{ox2} = +0.77$ V) and **8a**/**8b** ($E_{ox1} = +0.52$ V; $E_{ox2} = +0.78$ V), which was in agreement with previously reported values for unsubstituted 2TV ($E_{ox1} = +0.54$ V; $E_{ox2} = +0.87$ V).[12,19] The chemically irreversible oxidation of 2TV precluded a clear evaluation of the electron-exchange processes for compounds **9**, **10**, **11**, and **12**. Moreover, the second reversible oxidation of the porphyrin(s) was close to those of the 2TVs, which also helped to make their assignments difficult. Nevertheless, the second half-wave oxidation peaks of compound **9** ($E = +0.53$ V) and **10** ($E = +0.58$ V) were reasonably assigned to the first oxidation of 2TV by comparison with their respective 2TV models (**5**: $E = +0.52$ V and **8a**/**8b**: $E = +0.52$ V). Interestingly, in OSWV, the intensity of the first oxidation peak of 2TV was roughly half of the expected value compared to those of the porphyrin (reversible) in compound **9**, owing to an average value for the irreversible half-wave in OSWV. In compounds **11** and **12**, the first oxidation of 2TV was more difficult to ascribe. The OSWVs and CVs seemed to show a third irreversible oxidation peak as a small shoulder at around +0.9 V. By comparison with the values obtained for compounds **5**–**10**, it was reasonable to suppose that they should belong to the second irreversible oxidation (assigned to the 2TV unit) with positive shifts of about 0.13–0.16 V. Based on this hypothesis, the first oxidation potential should also be shifted at much higher potential (around +0.7 V) than compounds **5**–**10** (0.53–0.58 V). As the second oxidation of the porphyrin moiety in compounds **11** and **12** occurred at +0.71 V and +0.74 V, respectively, we suggested that the first irreversible oxidation of the 2TV bridge in compounds **11** and **12** must be overlapped by the second reversible oxidation of the porphyrin(s). These positive shifts in the oxidation of the 2TV bridge ($\Delta V \approx +0.15$ V) in C_{60}-based derivatives **11** and **12**, compared to their reference compounds without C_{60}, were coherent with similar observations for other fulleropyrrolidine–*n*TV derivatives reported by ourselves[18] and others.[9a,19] Indeed, it has previously been well-established that the introduction of a fulleropyrrolidine moiety at one tip of *n*TVs causes important positive-shifts of its oxidation potentials when compared to unsubstituted *n*TV. This behavior has been explained by two main reasons: First, the presence of bulky groups, such as fulleropyrrolidine (and porphyrins in our cases), hinders the approach of 2TV onto the electrode surface, thus leading to higher oxidation potentials for the 2TV moiety; and second, the lower coefficient diffusion in solution of the fullerene derivatives. Finally, we also suggest, as we had previously reported for other similar derivatives,[18] that the relative close contact between the 2TV moiety and the C_{60} cage should allow for π–π stacking interactions. Therefore, the withdrawing effect of the directly linked fulleropyrrolidine toward the 2TV bridge should also contribute to the increase in its oxidation potentials in compounds **11** and **12**. These potentials suggested that the radical cation (in photoinduced-electron-transfer processes) must be located in the porphyrins with the TV acting as a bridge. The experimentally determined HOMO–LUMO gap for compound **12** was 1.44 eV.

The UV/Vis absorption properties of compounds **11** and **12** were studied in toluene, CH_2Cl_2, and benzonitrile. The absorption spectra of compounds **11** and **12** in CH_2Cl_2 are shown in Figure 3. These spectra showed the characteristic Zn^{II}–porphyrin absorption bands: a Soret band at 430 nm and two Q bands at around 550 and 590 nm. Furthermore, the typical absorption of the fulleropyrrolidine in the UV region was also distinguishable. However, the absorption bands of the 2TV moiety were more difficult to distinguish

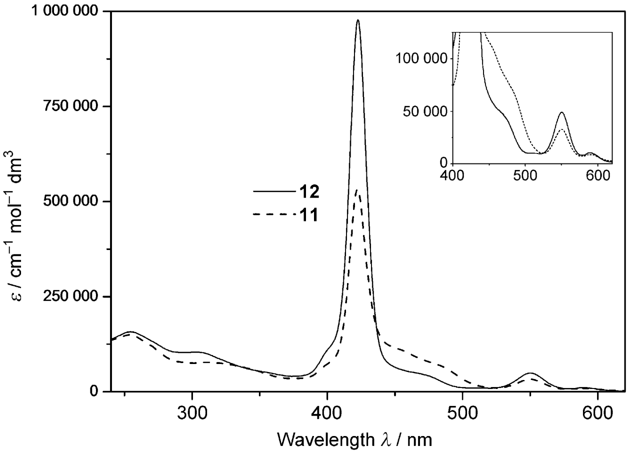

Figure 3. UV/Vis spectra of Por-2TV-C_{60} (**11**) and $(Por)_2$-2TV-C_{60} (**12**) in CH_2Cl_2.

because they were mostly overlapped by the intense Soret band of the porphyrin(s) (15–30 times more-intense). For 2TV reference derivatives **5** and **8a**/**8b**, two absorption bands were observed at around 340 and 390 nm. These bands appeared to be red-shifted in compounds **9**, **10**, **11**, and **12** in all of the solvents tested ($\Delta\lambda \approx 20$–60 nm); in particular, the 2TV band at around 460 nm was observed as a broad shoulder. The absorption coefficients of compounds **11** and **12** in CH_2Cl_2 were consistent with porphyrin/2TV/fullerene ratios of 1:1:1 and 2:1:1, respectively.

The fluorescence emission of $(Por)_2$-2TV-C_{60} (**12**) as well as its model compound (**10**) were studied in toluene and benzonitrile (Figure 4). Red-shifts of the Soret and Q bands of about 10 nm were observed in the emission/absorption spectra in benzonitrile compared to those in toluene or CH_2Cl_2 (see the Supporting Information, Figure SI.15). Such solvatochromism effects in polar solvents have been previously explained by the higher polarization of the ground electronic state for systems with covalently bridged spacers and strong electron-acceptors.[20]

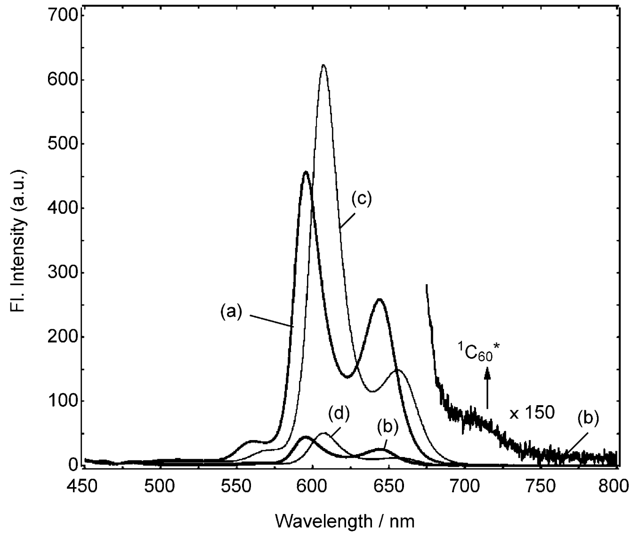

Figure 4. Room-temperature fluorescence spectra of Por_2-2TV (**10**) and $(Por)_2$-2TV-C_{60} (**12**) in photoexcited toluene (a and b, respectively) and benzonitrile (c and d, respectively) at 420 nm, with matching absorption at $\lambda_{ex} = 420$ nm.

The fluorescence spectra of $(Por)_2$-2TV-C_{60} (**12**) in toluene and in benzonitrile ($\lambda_{ex} = 420$ nm), along with those of reference compound $(Por)_2$-2TV (**10**), are shown in Figure 4. The fluorescence intensity of the porphyrin moiety (^{1}Por*; maxima at 600 and 650 nm in toluene) was markedly reduced (by a factor of at least 98 %) compared with that of compound **10** by the fullerene group on the opposite side of 2TV in compound **12**. In toluene, the appearances of the peaks at 715 nm owing to the fluorescence of fullerene indicated energy transfer from the ^{1}Por* moiety to the C_{60} moiety. In PhCN, a significant decrease in the fluorescence intensity was observed without the appearance of $^1C_{60}$* fluorescence. The fluorescence quantum yields (Φ) and lifetimes of compounds **9**–**12** are shown in Table 2, together with their fluorescence lifetimes (τ_f).

Table 2. Fluorescence quantum yields (Φ) and fluorescence lifetimes (τ_f) in PhCN and toluene.

Compound	PhCN		Toluene	
	Φ	τ_f [ns]	Φ	τ_f [ns]
Por-2TV (**9**)	0.031	1.7	0.038	1.8
$(Por)_2$-2TV (**10**)	0.033	1.5	0.035	1.5
Por-2TV-C_{60} (**11**)	0.006	–[a]	0.004	–[a]
$(Por)_2$-2TV-C_{60} (**12**)	0.006	–[a]	0.005	–[a]

[a] Too fast to determine accurately.

Photodynamics: First, the photodynamics of reference compound Ph-2TV (**5**) was examined by femtosecond laser flash photolysis. A transient absorption band at 755 nm, which was due to the singlet excited state of Ph-2TV (^{1}Ph-2TV*), was observed upon photoexcitation at 430 nm (Figure 5). The decay of the absorption band at 755 nm was accompanied by the generation of an absorption band at 600 nm, which was assigned to the triplet excited state of Ph-2TV (^{3}Ph-2TV*). The rate constant of intersystem crossing from ^{1}Ph-2TV* to ^{3}Ph-2TV* was determined from the decay of absorbance at 755 nm to be 3.9×10^9 s^{-1} ((260 ps)$^{-1}$) in PhCN at 298 K (Figure 5).

Next, the photodynamics of Por-2TV (**9**) was examined by femtosecond laser flash photolysis. Upon photoexcitation at 430 nm, a transient absorption band at 470 nm was observed, owing to the singlet excited state of the porphyrin moiety, together with a transient absorption band at 755 nm, which was due to the singlet excited state of the 2TV moiety (Figure 6a). The transient absorption band at 755 nm decayed much-more-rapidly than the reference compound (Ph-2TV) because of fast energy transfer from the singlet excited state of 2TV to the Por moiety (Figure 6a). The decay of the absorbance at 470 nm coincided with the appearance of an absorption band at 620 nm, which was due to the triplet excited state of the 2TV moiety (Figure 6a). This

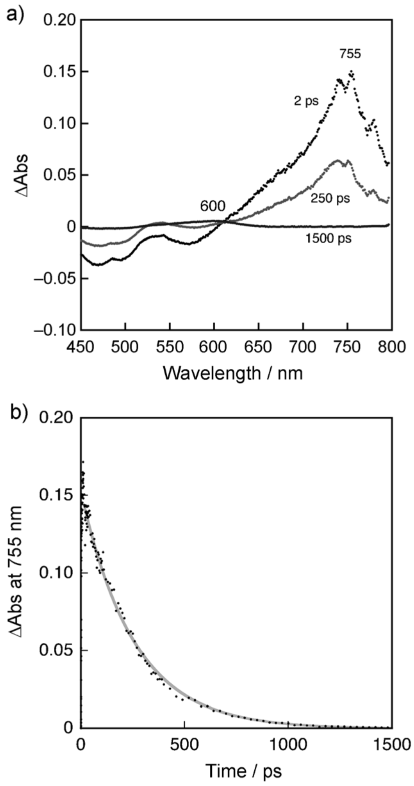

Figure 5. a) Transient absorption spectra of Ph-2TV (**5**) taken at 2, 250, and 1500 ps after femtosecond laser excitation at 430 nm in Ar-saturated PhCN; b) decay profile of the absorbance at 755 nm owing to ^{1}Ph-2TV*.

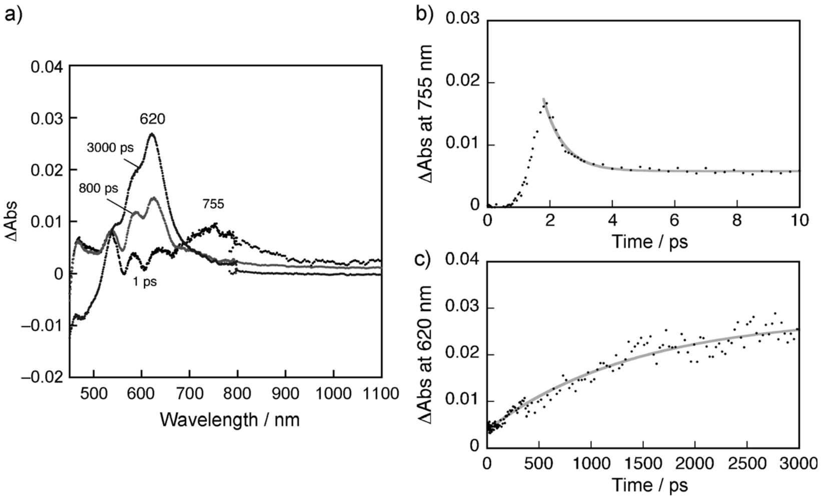

Figure 6. a) Transient absorption spectra of Por-2TV (**9**) taken at 1, 800, and 3000 ps after femtosecond laser excitation at 430 nm in Ar-saturated PhCN; b) decay profile of the absorbance at 755 nm; c) rise profile at 620 nm.

result indicated that the intersystem crossing from the singlet excited state to the triplet excited state of the porphyrin moiety was followed by rapid energy transfer from the porphyrin to the 2TV moiety to produce the triplet excited state of the 2TV moiety (Scheme 5). The rate constant of the energy transfer from ^{1}2TV* to Por and the intersystem crossing of Por were determined from the decay and rise-

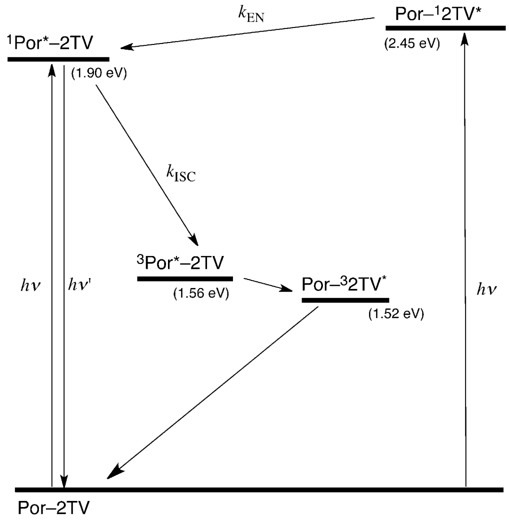

Scheme 5. Energy diagram for the photoinduced-energy-transfer processes of Por-2TV (**9**).

time profiles (Figure 6b,c) to be 1.5×10^{12} s^{-1} and 7.0×10^{8} s^{-1}, respectively.

When C_{60} was attached to the Por-2TV moiety (**9**) in Por-2TV-C_{60} (**11**), transient absorption bands at 740 and 1130 nm owing to $2TV^{•+}$ were observed, together with a transient absorption band at 1000 nm, which was due to $C_{60}^{•-}$, upon femtosecond laser excitation at 430 nm (Figure 7a). This assignment of the absorption bands at 740 and 1130 nm was confirmed by the absorption spectrum of $2TV^{•+}$, which was produced by the one-electron oxidation of Ph-2TV (**5**) with $[Ru(bpy)_3]^{3+}$ (Figure 8), although both absorption maxima were slightly blue-shifted. The time profiles of the absorbances at 1130 nm (Figure 7b) and 740 nm (Figure 7c) showed the formation and decay of the charge-separate state (Por-$2TV^{•+}$-$C_{60}^{•-}$). The rate constant of formation of $2TV^{•+}$ (2.0×10^{12} s^{-1} ((0.5 ps)$^{-1}$), as determined from the decay profile of the absorbance at 740 nm (Figure 7c), was much faster than the rate constant of formation of ^{3}TV* from the intersystem crossing of ^{1}Por* and the energy transfer from ^{3}Por* to 2TV in Figure 5b ((260 ps)$^{-1}$). This result indicated that energy transfer from ^{1}Por* to C_{60} was much faster than electron transfer from ^{1}Por* to C_{60} and the intersystem crossing. As a result, the electron transfer from 2TV to $^1C_{60}$* occurred to produce $2TV^{•+}$ and $C_{60}^{•-}$. Thus, the CS state of Por-$2TV^{•+}$-$C_{60}^{•-}$ was produced, rather than $Por^{•+}$-2TV-$C_{60}^{•-}$, despite the higher energy of Por-$2TV^{•+}$-$C_{60}^{•-}$ (1.61 eV versus 1.42 eV). The decay time profile

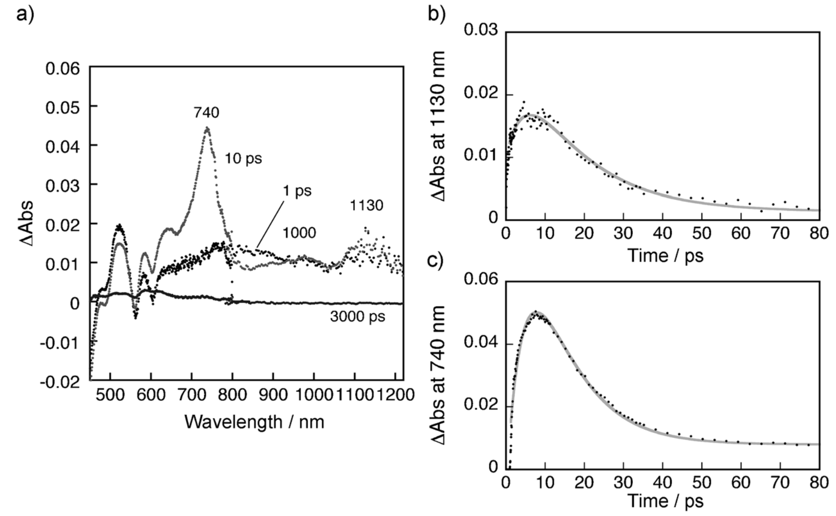

Figure 7. a) Transient absorption spectra of Por-2TV-C_{60} (**11**) taken at 1, 10, and 3000 ps after femtosecond laser excitation at 430 nm in Ar-saturated PhCN; time profiles of absorbance at b) 1130 and c) 740 nm.

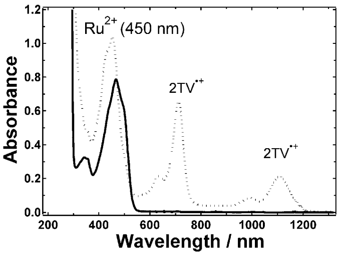

Figure 8. Absorption spectra of Ph-2TV (**5**; solid line) and Ph-2TV$^{\bullet+}$ (dashed line) from the one-electron oxidation of Ph-2TV (2.7×10^{-5} M) with $[Ru(bpy)_3](PF_6)_3$ (2.7×10^{-5} M) in CH_2Cl_2.

of the absorbance at 740 nm (Figure 7 c) afforded the rate constant of back-electron transfer from $C_{60}^{\bullet-}$ to 2TV$^{\bullet+}$ ($6.4\times10^{10}\,s^{-1}$ ((16 ps)$^{-1}$)).

The back-electron transfer mainly afforded ^{3}2TV*, as confirmed by the transient absorption band at 600 nm that was observed upon nanosecond laser excitation at 355 nm (Figure 9). No observation of the CS state of Por$^{\bullet+}$-2TV-$C_{60}^{\bullet-}$ indicated that the back-electron transfer to the triplet excited state was also much faster than electron transfer from Por to 2TV$^{\bullet+}$ to produce Por$^{\bullet+}$-2TV-$C_{60}^{\bullet-}$. The decay of the absorbance at 600 nm, which was due to ^{3}2TV* in Por-2TV-C_{60} (**11**), was significantly faster than the decay of ^{3}2TV* in Por-2TV (**9**; Figure 10). The acceleration of the decay of ^{3}2TV* with C_{60}, with a rate constant of $7.2\times10^{5}\,s^{-1}$ ((1.3 μs)$^{-1}$), as compared to the rate constant without C_{60} ((5.9 μs)$^{-1}$), suggested that electron transfer from Por to ^{3}2TV* occurred but that the back-electron transfer from $C_{60}^{\bullet-}$ to Por$^{\bullet+}$ was much faster than the decay of ^{3}2TV* to the ground state. This result was in sharp contrast to that of triad Por-2TV-C_{60} without a phenylethynyl bridge (Scheme 6), which afforded a relatively long-lived CT state of Por$^{\bullet+}$-2TV-$C_{60}^{\bullet-}$.[9d] Thus, the introduction of the phenylethynyl bridge resulted in the acceleration of the energy transfer from Por to C_{60}, but retarded

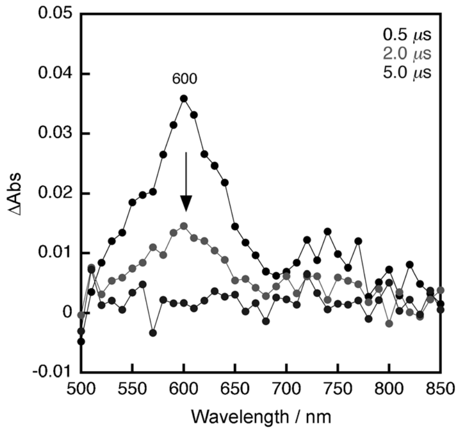

Figure 9. Transient absorption spectra of Por-2TV-C_{60} (**11**) upon nanosecond laser excitation at 490 nm in Ar-saturated PhCN.

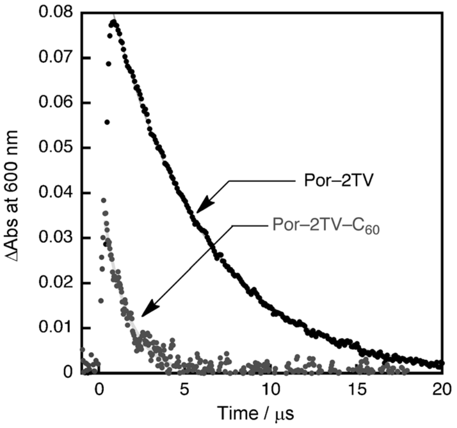

Figure 10. Decay profiles of absorbance at 600 nm owing to ^{3}2TV* in Por-2TV-C_{60} (**11**; gray) and Por-2TV (**9**; black) upon nanosecond laser excitation in Ar-saturated PhCN.

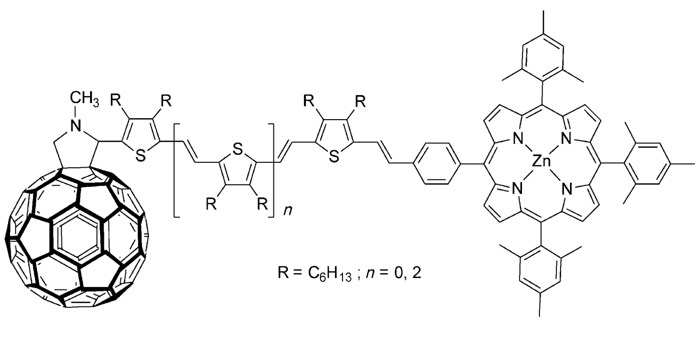

Scheme 6. The Por-2TV–C_{60} triad without a phenylethynyl bridge.

the electron transfer from Por to C_{60}. Moreover, the back-electron transfer from $C_{60}^{\bullet -}$ to $Por^{\bullet +}$ was also enhanced by the phenylethynyl bridge. The increased distance between Por and C_{60} with the phenylethynyl bridge resulted in an increase in the solvent-reorganization energy of electron transfer, which led to an increase in the back-electron transfer in the Marcus-inverted region.[6a,21]

Similar photodynamics was observed for $(Por)_2$-2TV-C_{60} tetrad (**12**; Figure 11). The formation of $2TV^{\bullet +}$ and $C_{60}^{\bullet -}$ through electron transfer from 2TV to $^1C_{60}$*, following energy transfer from ^{1}Por* to C_{60}, was clearly seen in the transient absorption spectra upon femtosecond laser excitation (Figure 11), as was the case with the Por-2TV-C_{60} triad (Figure 7). The back-electron transfer from $C_{60}^{\bullet -}$ to $2TV^{\bullet +}$ also afforded ^{3}2TV* ($\lambda_{max} = 600$ nm; see the transient absorption at 3 ns, Figure 5) and $^3C_{60}$* ($\lambda_{max} = 700$ nm), with a rate constant of $(17\ ps)^{-1}$ (Figure 11b), which was the same order as that of Por-2TV-C_{60} because the geometry between 2TV and C_{60} was the same as that between the $(Por)_2$-2TV-C_{60} tetrad and the Por-2TV-C_{60} triad. The light-harvesting efficiency of the $(Por)_2$-2TV-C_{60} tetrad was higher than that of Por-2TV-C_{60} because of the higher extinction coefficient (Figure 3).

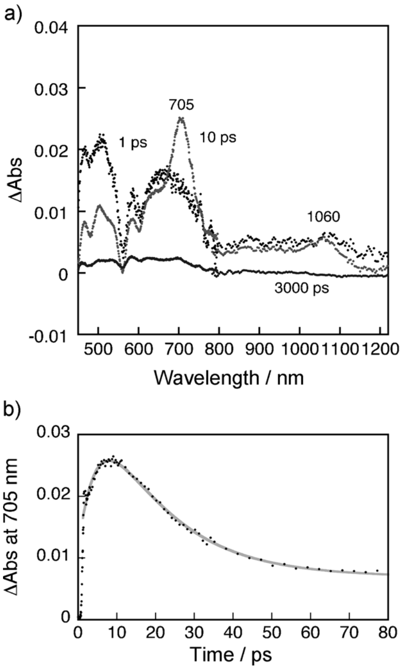

Figure 11. Transient absorption spectra of $(Por)_2$-2TV-C_{60} (**12**) in Ar-saturated PhCN after femtosecond laser excitation at 430 nm; b) time profile at 705 nm.

The energy diagram is summarized in Scheme 7. The energy levels of the singlet excited states of $^1C_{60}$*, ^{1}2TV*, and ^{1}Por* in Por-2TV-C_{60} were evaluated from the absorption and fluorescence peaks. The triplet states of C_{60}, 2TV, and Por have been evaluated previously from their weak phosphorescence peaks.[9] Upon photoexcitation of Por-2TV-C_{60}, energy transfer from ^{1}Por* to C_{60} occurred (rather than electron transfer from ^{1}Por* to C_{60}), followed by electron transfer from 2TV to $^1C_{60}$* to produce the CS state of Por-$2TV^{\bullet +}$-$C_{60}^{\bullet -}$. Although the energy of the CS state of $Por^{\bullet +}$-2TV-$C_{60}^{\bullet -}$ was lower than that of Por-$2TV^{\bullet +}$-$C_{60}^{\bullet -}$, back-electron transfer from $C_{60}^{\bullet -}$ to $2TV^{\bullet +}$ occurred to produce ^{3}2TV* rather than electron transfer from Por to $2TV^{\bullet +}$, because of the longer distance between Por and 2TV owing to the phenylethynyl bridge. Energy transfer from ^{3}2TV* to C_{60} occurred to afford $^3C_{60}$*, followed by electron transfer from Por to $^3C_{60}$* to produce $Por^{\bullet +}$-2TV-$C_{60}^{\bullet -}$, in which back-electron transfer from $C_{60}^{\bullet -}$ to $Por^{\bullet +}$ occurred much-more-rapidly than the triplet decay to the ground state (Scheme 7).

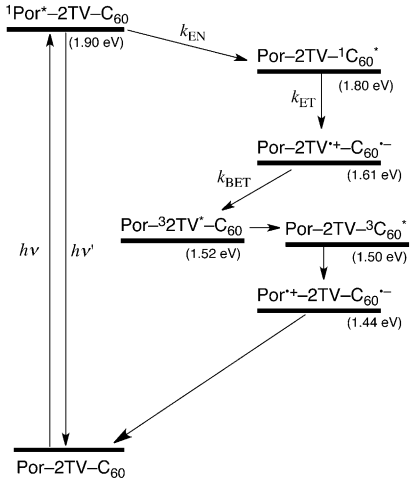

Scheme 7. Energy diagram for the photoinduced processes of Por-2TV-C_{60} (**11**) and $(Por)_2$-2TV-C_{60} (**12**).

Conclusion

We have synthesized new electron donor–acceptor triad (**11**: Por-2TV-C_{60}) and tetrad molecules (**12**: $(Por)_2$-2TV-C_{60}). $(Por)_2$-2TV-C_{60} had strong absorption bands owing to the two independent porphyrin moieties. The introduction of the phenylethynyl bridge in Por-2TV-C_{60} and $(Por)_2$-2TV-C_{60} resulted in drastic changes in their photodynamics, owing to a switch from electron transfer from ^{1}Por* to C_{60} in the compound without the phenylethynyl bridge (Scheme 6) to energy transfer from ^{1}Por* to C_{60}, thereby leading to the formation of the CS state of Por-$2TV^{\bullet +}$-$C_{60}^{\bullet -}$, which had higher energy than the CS state of $Por^{\bullet +}$-2TV-$C_{60}^{\bullet -}$. Thus, the porphyrin units in $(Por)_2$-2TV-C_{60} acted as a more-efficient photosensitizer than that in Por-2TV-C_{60} for the charge separation between 2TV and C_{60}. This study provides a new photosensitization strategy to afford the charge-separated state of $2TV^{\bullet +}$ and $C_{60}^{\bullet -}$, which was higher in energy than the charge-separated state of $Por^{\bullet +}$ and $C_{60}^{\bullet -}$.

Experimental Section

Synthesis of (*E*,*E*)-9: Compound (*E*,*E*)-**5** (47.6 mg, 69.7 μmol, 1 equiv), (A_3B) iodo–zinc porphyrin[14] (89 mg, 95.7 μmol, 1.4 equiv), $AsPh_3$ (30 mg, 90.0 μmol, 1.4 equiv), and $[Pd_2(dba)_3]$ (11 mg, 12.0 μmol, 0.2 equiv) were successively added into a Schlenk tube. Three cycles of argon/vacuum were then performed. Toluene (40 mL) and Et_3N (8 mL) were successively introduced via a cannula and the mixture was vigorously stirred at room temperature for three days. After evaporation of solvents, the crude mixture was filtrated through a small amount of SiO_2 gel (toluene). The volume of the solution was reduced to 1 mL under reduced pressure and the mixture was purified by gel-permeation chromatography (toluene), followed by two successive purifications by column chromatography on silica gel (*n*-hexane/CH_2Cl_2/Et_3N, 7:3:0.01) to afford compound (*E*,*E*)-**9** as a dark-purple solid in 66% yield (68.6 mg, 46.2 μmol). ^{1}H NMR ($CDCl_3$, 400 MHz) $\delta = 9.81$ (s, 1H), 8.92 (d, 2H, $^{3}J = 4.4$ Hz), 8.82 (d, 2H, $^{3}J = 4.4$ Hz), 8.75 (s, 4H), 8.29 (d, 2H, $^{3}J = 7.6$ Hz), 7.98 (d, 2H, $^{3}J = 7.6$ Hz), 7.72 (d, 2H, $^{3}J = 7.9$ Hz), 7.59 (d, 2H, $^{3}J = 7.9$ Hz), 7.39 (d, 1H, $^{3}J_{trans} = 15.9$ Hz), 7.33 (m, 6H), 7.30 (d, 1H, $^{3}J_{trans} = 15.8$ Hz), 7.07 (d, 1H, $^{3}J_{trans} = 15.8$ Hz), 7.02 (d, 1H, $^{3}J_{trans} = 15.9$ Hz), 2.88 (t, 2H, $^{3}J = 7.5$ Hz), 2.68 (br s, 15H), 1.92 (s, 18H), 1.62 (m, 8H), 1.56–1.35 (m, 24H), 1.06–0.86 ppm (m, 12H); ^{13}C NMR (APT, $CDCl_3$, 100 MHz) $\delta = 181.7$, 153.0, 150.0, 149.8, 149.6, 147.1, 143.9, 143.2, 142.6, 141.6, 139.3, 139.04, 138.95, 137.41, 137.35, 136.5, 134.73, 134.67, 134.5, 132.1, 131.8, 131.2, 131.1, 130.8, 129.8, 127.8, 127.6, 126.3, 123.7, 122.3, 121.1, 119.2, 118.9, 118.8, 118.6, 90.8, 90.6, 32.3, 31.7, 31.61, 31.55, 31.50, 31.4, 31.1, 29.7, 29.43, 29.36, 29.33, 27.23, 27.16, 27.1, 26.4, 22.65, 22.57, 21.8, 21.7, 21.5, 14.18, 14.11, 14.05 ppm; UV/Vis (CH_2Cl_2): λ_{max} (ε) = 300.5 (40800), 357.5 (26500), 422 (464300), 465.5 (76400), 549.5 (26800), 590 nm (5480 $dm^3\,mol^{-1}\,cm^{-1}$); MS (MALDI-TOF): *m*/*z* calcd. (%) for $C_{98}H_{106}N_4S_2OZn$: 1483.71 (87), 1484.71 (100), 1485.73 (82); found: 1483.95 (93), 1484.92 (100), 1485.89 (95) $[M]^+$.

Synthesis of (*E*,*E*)-10: Compound (*E*,*E*)-**10** was prepared according to the same procedure as compound **9**, from a mixture of (*E*,*E*)-**8a**/**8b** (150 mg; 77 mol%, 160 μmol bis-alkyne (*E*,*E*)-**8a** and 23 mol%, 47.9 μmol mono-alkyne (*E*,*E*)-**8b**), [5-*p*-iodophenyl-10,15,20-tris-(2,4,6-trimethylphenyl) zinc porphyrin][14] (500 mg, 537 μmol), $AsPh_3$ (30 mg, 212 μmol), $[Pd_2(dba)_3]$ (60 mg, 65.5 μmol), in toluene (80 mL) and Et_3N (16 mL). After evaporation of the solvents, the crude product was filtered through a small plug of silica gel (toluene). The volume of the solution was reduced to 1 mL and the mixture was purified by gel permeation chromatography. The first major band that contained (*E*,*E*)-**10** was purified twice more by gel permeation chromatography and three times by column chromatography on silica gel (*n*-hexane/$CHCl_3$/Et_3N, 5:5:0.01) to afford (*E*,*E*)-**10** (329 mg, 142 μmol) as a dark-purple solid in 89% yield (based on the effective amount of starting (*E*,*E*)-**8a**). ^{1}H NMR ($CDCl_3$, 400 MHz) $\delta =$ 9.66 (s, 1H), 8.98 (d, 4H, $^{3}J = 4.6$ Hz), 8.87 (d, 4H, $^{3}J = 4.6$ Hz), 8.80 (s, 8H), 8.35 (d, 4H, $^{3}J = 7.8$ Hz), 8.06 (d, 4H, $^{3}J = 7.8$ Hz), 7.98 (s, 1H), 7.90 (s, 2H), 7.52 (d, 1H, $^{3}J_{trans} = 15.8$ Hz), 7.34 (d, 1H, $^{3}J_{trans} = 15.8$ Hz), 7.35 (s, 8H), 7.34 (s, 4H), 7.10 (2×d, 2H, $^{3}J_{trans} = 15.8$ Hz), 2.84 (2×qt, 4H, $^{3}J = 7.5$ Hz), 2.69 (br s, 22H), 1.93 (s, 36H), 1.75–1.30 (m, 32H), 1.09–0.91 ppm (m, 12H); ^{13}C NMR (APT, $CDCl_3$, 100 MHz) $\delta = 181.6$, 153.02, 152.97, 150.03, 150.01, 149.8, 149.6, 147.1, 143.9, 143.6, 143.0, 141.7, 139.3, 139.1, 139.0, 138.1, 137.4, 136.2, 135.0, 134.65, 134.56, 133.6, 131.9, 131.25, 131.17, 130.8, 129.9, 129.3, 127.7, 126.9, 124.4, 123.7, 122.1, 121.9, 119.1, 119.0, 118.85, 118.77, 90.5, 89.5, 32.2, 31.74, 31.69, 31.65, 31.55, 31.4, 31.2, 29.7, 29.48, 29.46, 29.36, 27.29, 27.17, 26.5, 22.72, 22.67, 22.6, 21.8, 21.7, 21.5, 14.2, 14.11, 14.05 ppm; UV/Vis (CH_2Cl_2): λ_{max} (ε) = 279 (50500), 422.5 (683000), 456.5 (40750), 550 (33100), 590 nm (6 290 $dm^3\,mol^{-1}\,cm^{-1}$); MS (MALDI-TOF): *m*/*z* calcd (%) for $C_{153}H_{150}N_8OS_2Zn_2$: 2312.00 (100), 2313.00 (97.8); found: 2312.44 $[M]^+$.

Synthesis of 11: A solution of (*E*,*E*)-**9** (30.5 mg, 20.5 μmol, 1 equiv), sarcosine (45.5 mg, 511 μmol, 25 equiv), and C_{60} (45.5 mg, 63.2 μmol, 3 equiv) in chlorobenzene (40 mL) was thoroughly degassed by bubbling through argon for 30 min. The solution was then heated to reflux for 12 h under an argon atmosphere. After cooling to room temperature, chlorobenzene was removed under reduced pressure and the crude mixture was dissolved in a minimum amount of CS_2 and purified by column chromatography on silica gel, first eluting with CS_2 to remove any unreacted C_{60}, then with toluene to recover a mixture of products. After evaporation of solvents, the crude product was purified by gel permeation chromatography (toluene) and twice by column chromatography on silica gel (CS_2/CH_2Cl_2, 10:1). Compound **11** was obtained as a glassy dark-purple solid in 81% yield (37.0 mg, 16.6 μmol). ^{1}H NMR ($CDCl_3$, 400 MHz) $\delta = 8.91$ (d, 2H, $^{3}J = 4.6$ Hz), 8.80 (d, 2H, $^{3}J = 4.6$ Hz), 8.74 (s, 4H), 8.25 (d, 2H, $^{3}J = 8$ Hz), 7.95 (d, 2H, $^{3}J = 8$ Hz), 7.67 (d, 2H, $^{3}J = 8.3$ Hz), 7.54 (d, 2H, $^{3}J = 8.3$ Hz), 7.34 (d, 1H, $^{3}J_{trans} = 15.8$ Hz), 7.30 (br s, 6H), 7.06 (s, 2H), 6.92 (d, 1H, $^{3}J_{trans} = 15.8$ Hz), 5.33 (s, 1H), 4.97 (d, 1H, $^{2}J = 9.5$ Hz), 4.22 (d, 1H, $^{2}J = 9.5$ Hz), 2.95 (s, 3H), 2.81 (t, 2H, $^{3}J = 7.5$ Hz), 2.64 (br s, 15H), 1.88 (s, 18H), 1.65–1.26 (m, 32H), 0.99–0.87 ppm (m, 12H); ^{13}C NMR (APT, $CDCl_3$, 100 MHz) $\delta = 155.8$, 153.9, 153.2, 153.1, 150.0, 149.9, 149.8, 149.6, 147.0, 146.5, 146.2, 146.1, 146.0, 145.9, 145.81, 145.75, 145.6, 145.3, 145.2, 145.1, 145.0, 144.9, 144.39, 144.36, 144.0, 143.2, 143.1, 142.9, 142.7, 142.6, 142.35, 142.28, 142.1, 141.9, 141.81, 141.76, 141.7, 141.4, 140.3, 140.0, 139.9, 139.6, 139.30, 139.28, 139.02, 138.95, 137.9, 137.7, 137.4, 137.1, 136.5, 135.9, 135.3, 134.6, 134.5, 132.8, 132.1, 131.9, 131.2, 131.1, 130.7, 129.8, 127.6, 126.7, 126.2, 122.4, 121.9, 121.3, 120.0, 119.5, 119.3, 119.0, 118.8, 90.7, 90.6, 77.8, 70.0, 68.9, 40.6, 31.8, 31.8, 31.7, 31.6, 31.41, 31.36, 29.6, 29.5, 29.4, 29.1, 27.9, 27.2, 26.9, 22.71, 22.70, 22.65, 21.82, 21.77, 21.5, 14.23, 14.20, 14.1; IR (KBr): $\tilde{\nu} = 2949$, 2918, 2850, 2777, 1460, 1333, 997, 799, 523 cm^{-1}; UV/Vis (CH_2Cl_2): λ_{max} (ε) = 254 (149000), 308.5 (81600), 422 (532000), 550 (31100), 590 nm (7570 $dm^3\,mol^{-1}\,cm^{-1}$); MS (MALDI-TOF): *m*/*z* calcd (%) for $C_{160}H_{112}N_5OS_2$: 2232.77 (100), 2233.77 (98); found: 2233.04 $[M+H]^+$.

Synthesis of 12: Compound **12** was prepared according to the same procedure as described for compound **11**, from a solution of (*E*,*E*)-**10** (50.4 mg, 21.8 μmol, 1 equiv), sarcosine (59.0 mg, 662 μmol, 30 equiv), and C_{60} (58.9 mg, 81.8 μmol, 4 equiv) in chlorobenzene (50 mL). After evaporation of chlorobenzene under reduced pressure, the crude mixture was dissolved in a minimum amount of CS_2 and purified by column chromatography on silica gel, first eluting with CS_2 to remove any unreacted C_{60}, then with toluene to recover a mixture of products. After evaporation of the solvents, the crude material was purified twice by gel permeation chromatography (toluene) and twice by column chromatography on silica gel (CS_2/CH_2Cl_2, 8:2). Compound (*E*,*E*)-**12** was obtained as a glassy dark-purple product in 49% yield (32.5 mg, 10.6 μmol). ^{1}H NMR ($CDCl_3$, 400 MHz) $\delta = 8.94$ (d, 4H, $^{3}J = 4.6$ Hz), 8.82 (d, 4H, $^{3}J = 4.6$ Hz), 8.75 (s, 8H), 8.31 (d, 4H, $^{3}J = 7.8$ Hz), 8.02 (d, 4H, $^{3}J = 7.8$ Hz), 7.91 (s, 1H), 7.83 (s, 2H), 7.45 (d, 1H, $^{3}J_{trans} = 15.8$ Hz), 7.31 (s, 12H), 7.10 (s, 2H), 6.98 (d, 1H, $^{3}J_{trans} = 15.8$ Hz), 5.31 (s, 1H), 4.93 (d, 1H, $^{2}J = 9.7$ Hz), 4.20 (d, 1H, $^{2}J = 9.7$ Hz), 2.95 (s, 3H), 2.85–2.53 (m, 26H), 1.88 (s, 36H), 1.67–1.26 (m, 32H), 1.04–0.88 ppm (m, 12H); ^{13}C NMR (APT, $CDCl_3$, 100 MHz) $\delta = 155.7$, 153.8, 153.15, 153.10, 150.0, 149.9, 149.8, 149.6, 146.89, 146.86, 146.4, 146.1, 146.0, 145.9, 145.8, 145.73, 145.72, 145.6, 145.5, 145.24, 145.19, 145.14, 144.99, 144.97, 144.91, 144.8, 144.3, 144.2, 144.0, 143.9, 143.4, 143.2, 142.9, 142.8, 142.6, 142.3, 142.23, 142.20, 142.1, 141.96, 141.85, 141.77, 141.74, 141.72, 141.69, 141.62, 141.3, 141.2, 140.4, 139.8, 139.7, 139.58, 139.56, 139.3, 139.0, 138.9, 138.4, 137.9, 137.4, 137.1, 136.4, 136.0, 135.4, 135.2, 134.6, 134.3, 133.3, 132.9, 131.9, 131.2, 131.1, 130.8, 129.9, 129.2, 127.7, 125.8, 124.2, 122.1, 122.0, 120.1, 119.5, 119.2, 119.0, 118.8, 90.3, 89.6, 77.8, 70.0, 68.8, 40.6, 31.8, 31.74, 31.69, 31.59, 31.44, 31.39, 29.7, 29.6, 29.49, 29.46, 29.1, 27.9, 27.2, 27.0, 22.72, 22.69, 22.66, 21.8, 21.7, 21.5, 14.23, 14.22, 14.20 ppm; FTIR (KBr): $\tilde{\nu} = 2951$, 2921, 2853, 1459, 1204, 999, 798, 723, 527 cm^{-1}; UV/Vis (CH_2Cl_2): λ_{max} (ε) = 255 (163000), 301 (109000), 422.5 (978000), 550 (48000), 590 nm (9930 $dm^3\,mol^{-1}\,cm^{-1}$); MS (MALDI-TOF): *m*/*z* calcd (%) for $C_{215}H_{156}N_9S_2Zn_2$: 3059.05 (94), 3060.05 (100), 3061.05 (95); found: 3059.12 (94), 3060.08 (100), 3061.10 (96) $[M+H]^+$.

Acknowledgements

Financial support from the Ministerio de Ciencia y Tecnología of Spain, FEDER funds (Project CTQ2010–17498), the Consolider Project HOPE, and the JJCC de Castilla-La Mancha (Project PEII11–0195–1214), a Grant-in-Aid (Nos. 20108010 and 23750014) and the Global COE program “Global Education and Research Center for Bio-Environmental Chemistry” of Osaka University from the Ministry of Education, Culture, Sports, Science and Technology, Japan, and from the KOSEF/MEST through the WCU project (R31–2008–000–10010–0) are gratefully acknowledged.

---

[1] a) H. B. Gray, *Nat. Chem.* **2009**, *1*, 7; b) J. L. Dempsey, B. S. Brunschwig, J. R. Winkler, H. B. Gray, *Acc. Chem. Res.* **2009**, *42*, 1995–2004; c) N. S. Lewis, D. G. Nocera, *Proc. Natl. Acad. Sci. USA* **2006**, *103*, 15729–15735; d) V. Balzani, A. Credi, M. Venturi, *ChemSusChem* **2008**, *1*, 26–58; e) S. Fukuzumi, *Eur. J. Inorg. Chem.* **2008**, 1351–1362.

[2] a) D. Gust, T. A. Moore, A. L. Moore, in *Electron Transfer in Chemistry, Vol. 3* (Ed.: V. Balzani), Wiley-VCH, Weinheim, **2001**, 272–336; b) D. Gust, T. A. Moore, A. L. Moore, *Acc. Chem. Res.* **2009**, *42*, 1890–1898; c) D. M. Guldi, M. Prato, *Acc. Chem. Res.* **2000**, *33*, 695–703; d) D. M. Guldi, *Nature Nanotech.* **2008**, *3*, 257–258; e) G. Bottari, G. de La Torre, D. M. Guldi, T. Torres, *Chem. Rev.* **2010**, *110*, 6768–6816; f) V. Sgobba, D. M. Guldi, *J. Mater. Chem.* **2008**, *18*, 153–157; g) N. Martin, L. Sanchez, M. A. Herranz, B. Illescas, D. M. Guldi, *Acc. Chem. Res.* **2007**, *40*, 1015–1024; h) M. R. Wasielewski, *Acc. Chem. Res.* **2009**, *42*, 1910–1921; i) S. Fukuzumi, *Org. Biomol. Chem.* **2003**, *1*, 609–620; j) S. Fukuzumi, T. Kojima, *J. Mater. Chem.* **2008**, *18*, 1427–1439; k) S. Fukuzumi, *Bull. Chem. Soc. Jpn.* **2006**, *79*, 177–195; l) S. Fukuzumi, *Phys. Chem. Chem. Phys.* **2008**, *10*, 2283–2297.

[3] a) H. Imahori, D. M. Guldi, K. Tamaki, Y. Yoshida, C. Luo, Y. Sakata, S. Fukuzumi, *J. Am. Chem. Soc.* **2001**, *123*, 6617–6628; b) S. Fukuzumi, K. Ohkubo, H. Imahori, J. Shao, Z. Ou, G. Zheng, Y. Chen, R. K. Pandey, M. Fujitsuka, O. Ito, K. M. Kadish, *J. Am. Chem. Soc.* **2001**, *123*, 10676–10683; c) K. Ohkubo, H. Imahori, J. Shao, Z. Ou, K. M. Kadish, Y. Chen, R. K. Pandey, M. Fujitsuka, O. Ito, S. Fukuzumi, *J. Phys. Chem. A* **2002**, *106*, 10991–10998; d) Y. Kashiwagi, K. Ohkubo, J. A. McDonald, I. M. Blake, M. J. Crossley, Y. Araki, O. Ito, H. Imahori, S. Fukuzumi, *Org. Lett.* **2003**, *5*, 2719–2721; e) K. Ohkubo, J. Shao, Z. Ou, K. M. Kadish, G. Li, R. K. Pandey, M. Fujitsuka, O. Ito, H. Imahori, S. Fukuzumi, *Angew. Chem.* **2004**, *116*, 871–874; *Angew. Chem. Int. Ed.* **2004**, *43*, 853–856; f) D. M. Guldi, F. Spänig, D. Kreher, I. F. Perepichka, M. R. Bryce, K. Ohkubo, S. Fukuzumi, *Chem. Eur. J.* **2008**, *14*, 250–258; g) F. D′Souza, R. Chita, K. Ohkubo, M. Tasior, N. K. Subbaiyan, M. E. Zandler, M. Rogacki, D. T. Gryko, S. Fukuzumi, *J. Am. Chem. Soc.* **2008**, *130*, 14263–14272.

[4] a) M. Urbani, J. Iehl, I. Osinska, R. Louis, M. Holler, J.-F. Nierengarten, *Eur. J. Org. Chem.* **2009**, 3715–3725; b) H. Yamada, H. Imahori, Y. Nishimura, I. Yamazaki, T. K. Ahn, S. K. Kim, D. Kim, Shunichi Fukuzumi, *J. Am. Chem. Soc.* **2003**, *125*, 9129–9139; c) T. Hasobe, Y. Kashiwagi, M. A. Absalom, K. Hosomizu, M. J. Crossley, H. Imahori, P. V. Kamat, S. Fukuzumi, *Adv. Mater.* **2004**, *16*, 975–979; d) T. Hasobe, H. Imahori, P. V. Kamat, T. K. Ahn, D. Kim, T. Hanada, T. Hirakawa, S. Fukuzumi, *J. Am. Chem. Soc.* **2005**, *127*, 1216–1228; e) M. Tanaka, K. Ohkubo, C. P. Gross, R. Guilard, S. Fukuzumi, *J. Am. Chem. Soc.* **2006**, *128*, 14625–14633; f) F. D′Souza, E. Maligaspe, P. A. Karr, A. L. Schumacher, M. E. Ojaimi, C. P. Gros, J.-M. Barbe, K. Ohkubo, S. Fukuzumi, *Chem. Eur. J.* **2008**, *14*, 674–681; g) S. Fukuzumi, K. Saito, K. Ohkubo, T. Khoury, Y. Kashiwagi, M. A. Absalom, S. Gadde, F. D′Souza, Y. Araki, O. Ito, M. J. Crossley, *Chem. Commun.* **2011**, *47*, 7980–7982.

[5] a) M. Carano, M. Marcaccio, M. F. Paolucci, *Three Electrodes and a Cage: An account of Electrochemical Research on C_{60}, C_{70} and their derivatives in Fullerenes-Principles and Applications* 2nd ed., (Eds.: F. Langa, J. F. Nierengarten), RSC, Cambridge, UK, **2012**; b) A. Satake, Y. Kobuke, *Org. Biomol. Chem.* **2007**, *5*, 1679–1691; c) M. Fujitsuka, M. Hara, S. Tojo, A. Okada, V. TroIani, N. Solladié, T. Majima, *J. Phys. Chem. B* **2005**, *109*, 33–35; d) M. Fujitsuka, D. W. Cho, N. Solladié, V. Troiani, H. Qiu, T. Majima, *J. Photochem. Photobiol. A* **2007**, *188*, 346–350.

[6] F. D′Souza, R. Chita, K. Ohkubo, M. Tasior, N. K. Subbaiyan, M. E. Zandler, M. Rogacki, D. T. Gryko, S. Fukuzumi, *J. Am. Chem. Soc.* **2008**, *130*, 14263–14272.

[7] a) F. D′Souza, E. Maligaspe, K. Ohkubo, M. E. Zandler, N. K. Subbaiyan, S. Fukuzumi, *J. Am. Chem. Soc.* **2009**, *131*, 8787- 8797; b) M. E. El-Khouly, J. H. Kim, K.-Y. Kay, C. S. Choi, O. Ito, *Chem. Eur. J.* **2009**, *15*, 5301–5310; c) K. Ohkubo, S. Fukuzumi, *J. Porphyrins Phthalocyanines* **2008**, *12*, 993–1004; d) F. D′Souza, O. Ito, *Chem. Commun.* **2009**, 4913–4928; e) N. Armaroli, G. Accorsi in *Fullerenes: Principles and Applications*, (Eds.: F. Langa, J.-F. Nierengarten), RSC, Cambridge, **2007**, 79–126; f) S. Fukuzumi, K. Ohkubo, H. Imahori, D. M. Guldi, *Chem. Eur. J.* **2003**, *9*, 1585–1593; g) A. Takai, M. Chkounda, A. Eggenspiller, C. P. Gros, M. Lachkar, J.-M. Barbe, S. Fukuzumi, *J. Am. Chem. Soc.* **2010**, *132*, 4477–4489.

[8] a) G. R. Hutchison, M. A. Ratner, T. J. Marks, *J. Am. Chem. Soc.* **2005**, *127*, 16866–16881; b) G. R. Hutchison, M. A. Ratner, T. J. Marks, *J. Am. Chem. Soc.* **2005**, *127*, 2339–2350; c) T. Oike, T. Kurata, K. Takimiya, T. Otsubo, Y. Aso, H. Zhang, Y. Araki, O. Ito, *J. Am. Chem. Soc.* **2005**, *127*, 15372–15373.

[9] a) C. Martineau, P. Blanchard, D. Rondeau, J. Delaunay, J. Roncali, *Adv. Mater.* **2002**, *14*, 283–287; b) J. Roncali, *Acc. Chem. Res.* **2000**, *33*, 147–156; c) I. Jestin, P. Frère, P. Blanchard, J. Roncali, *Angew. Chem.* **1998**, *110*, 990–993; *Angew. Chem. Int. Ed.* **1998**, *37*, 942–945; d) F. Oswald, D.-M. Shafiqul Islam, Y. Araki, V. Troiani, R. Caballero, P. de La Cruz, O. Ito, F. Langa, *Chem. Commun.* **2007**, 4498–4500; e) J. Casado, S. Rodrìguez Gonzàlez, M. Carmen Ruiz Delgado, M. Moreno Oliva, J. T. López Navarrete, R. Caballero, P. de La Cruz, F. Langa, *Chem. Eur. J.* **2009**, *15*, 2548–2559; f) O. Ito, K. Yamanaka, *Bull. Chem. Soc. Jpn.* **2009**, *82*, 316.

[10] A. L. Thompson, T. S. Ahn, K. R. J. Thomas, S. Thayumanavan, T. J. Martínez, C. J. Bardeen, *J. Am. Chem. Soc.* **2005**, *127*, 16348–16349.

[11] E. Díez-Barra, J. C. García-Martínez, S. Merino, R. del Rey, J. Rodríguez-López, P. Sánchez-Verdú, J. Tejeda, *J. Org. Chem.* **2001**, *66*, 5664–5670.

[12] I. Jestin, P. Frère, N. Mercier, E. Levillain, D. Stievenard, J. Roncali, *J. Am. Chem. Soc.* **1998**, *120*, 8150–8158.

[13] The ratio was estimated by ^{1}H NMR spectroscopy.

[14] Synthesized according to a literature procedure in two steps from commercial 4-iodo-benzaldehyde (1 equiv), pyrrole (4 equiv), and 2,4,6-trimethylbenzaldehyde (3 equiv) under classical Lindsey conditions followed by metalation with $Zn(AcO)_2$; see reference [15a].

[15] a) J. S. Lindsey, R. W. Wagner, *J. Org. Chem.* **1989**, *54*, 828–836; b) K. Sonogashira, Y. Tohda, N. Hagihara, *Tetrahedron Lett.* **1975**, 4467; c) R. W. Wagner, Y. Ciringh, C. Clausen, J. S. Lindsey, *Chem. Mater.* **1999**, *11*, 2974; d) N. Srinivasan, C. A. Haney, J. S. Lindsey, W. Zhang, B. T. Chait, *J. Porphyrins Phthalocyanines*, **1999**, *3*, 283–291; e) S. Ik Yang, J. Li, H. Sun Cho, D. Kim, D. F. Bocian, D. Holten, J. S. Lindsey, *J. Mater. Chem.* **2000**, *10*, 283–296; f) S. Higashida, H. Imahori, T. Kaneda, Y. Sakata, *Chem. Lett.* **1998**, *7*, 605–606; g) F. Cattaruzza, A. Llanes-Pallas, A. G. Marrani, E. A. Dalchiele, F. Decker, R. Zanoni, M. Prato, D. Bonifazi, *J. Mater. Chem.* **2008**, *18*, 1570–1581.

[16] M. Prato, M. Maggini, *Acc. Chem. Res.* **1998**, *31*, 519–526.

[17] a) P. de La Cruz, A. de La Hoz, L. M. Font, F. Langa, M. C. Rodriguez, *Tetrahedron Lett.* **1998**, *39*, 6053; b) F. Ajamaa, T. M. Figueira Duarte, C. Bourgogne, M. Holler, P. W. Fowler, J.-F. Nierengarten, *Eur. J. Org. Chem.* **2005**, 3766–3774; c) J. N. Clifford, A. Gégout, S. Zhang, R. Pereira de Freitas, M. Urbani, M. Holler, P. Ceroni, J.-F. Nierengarten, N. Armaroli, *Eur. J. Org. Chem.* **2007**, 5899–5908.

[18] M. Urbani, B. Pelado, P. de La Cruz, K.-I Yamanaka, O. Ito, F. Langa, *Chem. Eur. J.* **2011**, *17*, 5432–5444.

[19] a) J. J. Apperloo, C. Martineau, P. A. van Hal, J. Roncali, R. A. J. Janssen, *J. Phys. Chem. A*,**2002**, *106*, 21–31; b) S.-G. Liu, C. Martineau, J.-M. Raimundo, J. Roncali, L. Echegoyen, *Chem. Commun.* **2001**, 913–914.

[20] D. Laage, W. H. Thompson, M. Blanchard-Desce, J. T. Hynes, *J. Phys. Chem. A* **2003**, *107*, 6032–6046.

[21] a) R. A. Marcus, *Angew. Chem.* **1993**, *105*, 1161–1172; *Angew. Chem. Int. Ed. Engl.* **1993**, *32*, 1111–1121; b) R. A. Marcus, N. Sutin, *Biochim. Biophys. Acta* **1985**, *811*, 265–322.

Received: July 22, 2011
Revised: February 17, 2012

Energy Transfer

M. Urbani, K. Ohkubo, D. M. S. Islam, S. Fukuzumi, F. Langa** . . . ■■■■–■■■■

Photoinduced Energy and Electron Transfer in Phenylethynyl-Bridged Zinc Porphyrin–Oligothienylenevinylene–C_{60} Ensembles

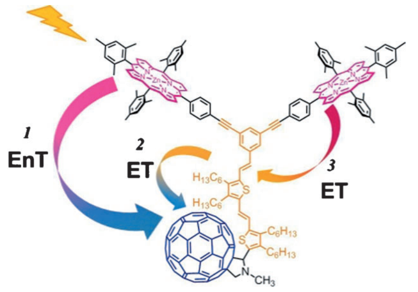

Bridge over troubled waters: Photoinduced charge separation occurred in an electron donor–bridge–acceptor tetrad, which incorporated C_{60} and two porphyrin groups that were covalently linked through a phenylethynyl oligothienylenevinylene bridge, by ultrafast energy transfer from the photoexcited porphyrin to C_{60} (EnT).